



## ISTITUTO NAZIONALE DI RICERCA METROLOGICA Repository Istituzionale

Fast TiO<sub>2</sub> sensitization using the semisquaric acid as anchoring group

*Original*

Fast TiO<sub>2</sub> sensitization using the semisquaric acid as anchoring group / Pugliese, Diego; Shahzad, Nadia; Sacco, Adriano; Musso, Guido; Lamberti, Andrea; G., Caputo; Tresso, Elena Maria; Bianco, Stefano; Pirri, Candido. - In: INTERNATIONAL JOURNAL OF PHOTOENERGY. - ISSN 1110-662X. - 2013:Article ID 871526(2013). [10.1155/2013/871526]

*Availability:*

This version is available at: 11696/77315 since:

*Publisher:*

Hindawi Publishing Corporation

*Published*

DOI:10.1155/2013/871526

*Terms of use:*

This article is made available under terms and conditions as specified in the corresponding bibliographic description in the repository

*Publisher copyright*

(Article begins on next page)

## Research Article

# Fast TiO<sub>2</sub> Sensitization Using the Semisquaric Acid as Anchoring Group

**D. Pugliese,<sup>1,2</sup> N. Shahzad,<sup>1,2</sup> A. Sacco,<sup>1</sup> G. Musso,<sup>3,4</sup> A. Lamberti,<sup>1,2</sup> G. Caputo,<sup>3,4</sup>  
E. Tresso,<sup>1,2</sup> S. Bianco,<sup>1</sup> and C. F. Pirri<sup>1,2</sup>**

<sup>1</sup> Center for Space Human Robotics @Polito, Istituto Italiano di Tecnologia, Corso Trento 21, 10129 Turin, Italy

<sup>2</sup> Applied Science and Technology Department, Politecnico di Torino, Corso Duca degli Abruzzi 24, 10129 Turin, Italy

<sup>3</sup> Chemistry Department and Nanostructured Interfaces and Surfaces Interdepartmental Center of Excellence, Università degli Studi di Torino, Via Giuria 7, 10125 Turin, Italy

<sup>4</sup> Cyanine Technologies S.p.A and Pianeta s.r.l., Via Giannone 3, 10036 Settimo Torinese, Italy

Correspondence should be addressed to D. Pugliese; [diego.pugliese@polito.it](mailto:diego.pugliese@polito.it)

Received 20 July 2013; Revised 6 September 2013; Accepted 10 September 2013

Academic Editor: Jun-Ho Yum

Copyright © 2013 D. Pugliese et al. This is an open access article distributed under the Creative Commons Attribution License, which permits unrestricted use, distribution, and reproduction in any medium, provided the original work is properly cited.

Metal-free dye molecules for dye-sensitized solar cells application can avoid some of the typical drawbacks of common metal-based sensitizers, that are high production costs, relatively low molar extinction coefficient in the visible region, limited availability of precursors, and waste disposal issues. Recently we have proposed an innovative organic dye based on a simple hemi-squaraine molecule (CT1). In the present work, the effect of the sensitization time of the TiO<sub>2</sub> photoelectrode in the dye solution is studied with the aim of optimizing the performance of CT1-based DSCs. Moreover, the addition of the chenodeoxycholic acid (CDCA) as coadsorbent in the dye solution at different concentrations is investigated. Both CT1-sensitized mesoporous TiO<sub>2</sub> photoanodes and complete solar cells have been fully characterized in their electrical and absorption properties. We have found that the best photoconversion performances are obtained with 1 hour of impregnation time and a 1 mM CDCA concentration. The very fast kinetics in dye adsorption, with optimal sensitization steps almost 15 times faster than conventional Ru-based sensitizers, confirms the theoretical predictions and indicates a strong interaction of the semisquaric acid group with the anatase surface. This result suggests that this small molecule can be a promising sensitizer even in a continuous industrial process.

## 1. Introduction

Dye-sensitized solar cells (DSCs) represent one of the most promising alternatives to the standard silicon-based solar cells, thanks to their low manufacturing costs, easy fabrication process, and environmental sustainability. Since the seminal paper of O'Regan and Grätzel in 1991 [1], many efforts have been made to increase and stabilize over time the photoconversion efficiency (PCE) of these third generation solar devices. DSCs are photoelectrochemical cells constituted by a nanocrystalline wide-band gap semiconductor film as anode (usually TiO<sub>2</sub>), a sensitizer, an electrolyte, a counterelectrode, and a transparent conducting substrate. Under sunlight irradiation, the dye molecules are photoexcited and ultrafast inject electrons into the conduction band of the semiconductor; the original state of the dye is subsequently restored by electron donation from the electrolyte, usually a solution

of an organic solvent (or a ionic liquid) containing the I<sub>3</sub><sup>-</sup>/I<sup>-</sup> redox couple. The iodide is regenerated by reduction of triiodide at the counterelectrode by means of a catalyst (usually Pt), the circuit being completed through an external load [2].

The sensitizer, with its key role played in collecting the solar radiation and photogenerating the current, has attracted a strong research effort in the DSC community, since the dye properties strictly affect the light harvesting efficiency and the overall photoconversion properties of the cell. Standard sensitizers in DSCs can be divided into organometallic (polypyridyl complexes of ruthenium and osmium, metal porphyrin, and phthalocyanine), organic (cyanine dye, D- $\pi$ -A) and inorganic (quantum dots) dyes. Over the last 20 years, ruthenium polypyridyl complexes have achieved power conversion efficiencies beyond 11% and have shown

good stability [3]. Even more recently an efficiency greater than 12% has been reported in a cosensitized (Zn-porphyrin plus organic dye) DSC [4]. Nevertheless, metal-based sensitizers exhibit some important limits: expensive synthesis process, relatively low molar extinction coefficient in the visible region, limited availability of precursors, and waste disposal issues. In this context metal-free organic dyes could present several advantages, being obtainable with simple, fast, and cost-effective synthetic approach and characterized by high molar extinction coefficients [5, 6]. In comparison to the Ru-based sensitizers, however, organic dyes exhibit lower conversion efficiencies, due to the formation of dye aggregates on the semiconductor surface and to their narrow light absorption bands in the visible region. Therefore, several efforts have been made to study organic dye molecules with broader spectral responses and with anchoring group that strongly binds to the nanocrystalline  $\text{TiO}_2$  surface, ensuring electron coupling with the substrate [7–10].

In our previous paper [11], a simple hemi-squaraine dye (CT1) was proposed as an effective sensitizer for  $\text{TiO}_2$  thanks to the quite fast attachment of squaric acid moiety anchoring group to the semiconductor surface, with the formation of a type II heterostructure [12], ensuring adiabatic electron transfer from the molecule to the oxide.

In this work we present an optimization procedure of the performance of CT1-based DSCs, fabricated using a customized microfluidic architecture [13]. To this purpose, an optical study (UV-Visible spectroscopy) of the CT1-sensitized mesoporous  $\text{TiO}_2$  photoanodes and a deep electrical analysis (Current-Voltage, External Quantum Efficiency, and Electrochemical Impedance Spectroscopy) of the complete solar cells have been carried out. The dye loading mechanism was first investigated by varying the dipping time of the  $\text{TiO}_2$  photoelectrode, showing a very fast sensitization kinetics. Moreover, the addition of the chenodeoxycholic acid (CDCA) as coadsorbent in the dye solution at different concentrations was investigated, showing a more efficient dye anchoring with the reduction of molecule aggregation. Even if the obtained photoconversion efficiency values are lower with respect to the traditionally employed Ru-based N719/ $\text{TiO}_2$  cells, the results, evidencing a fast attachment of the dye to the  $\text{TiO}_2$  surface, suggest that the use of CT1 can lead to a significant time reduction in a continuous industrial process.

## 2. Experimental Details

**2.1. Materials and Fabrication.** Fluorine-doped tin oxide (FTO)-covered glasses ( $7 \Omega/\text{sq}$ , Solaronix)  $2 \text{ cm} \times 2 \text{ cm}$  were cleaned in order to remove particulates on the surface, as well as traces of organic, ionic, and metallic impurities. The cleaning procedure is divided into the following 4 steps: ultrasonic bath in acetone for 10 minutes, soaking in 2-propanol for few seconds, bath in piranha solution ( $\text{H}_2\text{SO}_4 : \text{H}_2\text{O}_2$  3:1) for 10 minutes, and finally rinsing in deionized water and drying under nitrogen flow. Afterwards, in order to remove residual moistures on the surface, the glasses were placed on a hot plate for 2 minutes at  $100^\circ\text{C}$ . Subsequently, a circular-shaped

$\text{TiO}_2$  layer (Ti-Nanoxide D37, Solaronix) was deposited onto FTO-covered glasses with tape casting technique [14], dried at room temperature for half an hour, and finally placed on a hot plate at  $50^\circ\text{C}$  for 10 minutes. A sintering process in a muffle furnace (Nabertherm series L/LT-B180) at  $450^\circ\text{C}$  for 30 minutes enabled the formation of a nanoporous  $\text{TiO}_2$  film with a mean thickness of  $(8.5 \pm 0.5) \mu\text{m}$ , as measured by a profilometer (P.10 KLA-Tencor Profiler). In order to obtain an increase of the photovoltaic conversion efficiency, a second set of samples with slightly higher  $\text{TiO}_2$  film thickness ( $9.5 \pm 0.5 \mu\text{m}$ ) was fabricated and employed in the second part of the work, the one in which CDCA was used as coadsorbent. A  $\text{TiCl}_4$  post-treatment was performed by dipping the freshly sintered  $\text{TiO}_2$  films into a 50 mM  $\text{TiCl}_4$  solution at  $70^\circ\text{C}$  for 30 minutes, then rinsing in abundant deionized water and drying under nitrogen flow. After the post-treatment, the  $\text{TiO}_2$  films were again sintered at  $450^\circ\text{C}$  for 30 minutes [15].

Photoanodes were then soaked into a 0.17 mM hemi-squaraine dye acetonitrile solution for different time intervals (5 minutes, 30 minutes, 1 hour, 3 hours, and 5 hours) at  $70^\circ\text{C}$  and subsequently rinsed in pure acetonitrile solution to remove unabsorbed dye molecules. CT1 hemi-squaraine dye was synthesized following the procedure described by Cicero et al. [11]. The dye impregnation process was performed with particular care in order to avoid any sort of contamination of the dye solution. The absorption spectrum was checked before each loading step with the purpose of assessing the reliability of the dye solution preparation and the stability of the sensitizer powder; the solution was maintained at ambient temperature ( $21^\circ\text{C}$ ), and glass containers covered by an Al foil were used in order to avoid plastic contamination and to keep dark conditions. Eight photoanodes were prepared for each experiment, in order to ensure statistics for the results. Five of them were used to assemble DSCs and the remaining three for the optical characterization.

Moreover, chenodeoxycholic acid in different concentrations (1 mM, 10 mM, 14 mM, and 18 mM) was employed as coadsorbent in the dye solution in order to reduce the sensitizer aggregation at the semiconductor surface [16]. Firstly, the sensitization time was fixed to 1 hour. Then, it was extended to 3 hours for the three most promising CDCA concentrations (0 mM, 1 mM, and 10 mM) in order to verify if a longer loading time could lead to an improvement of the photoconversion efficiency of the solar cells.

The counterelectrodes were fabricated as previously reported [13]. Briefly, two small pinholes were drilled into FTO/glass substrates using powder blasting technology. Then the substrates were cleaned with the 4 steps described above and coated with a thin layer (about 5 nm) of Pt deposited by thermal evaporation.

DSCs were fabricated employing our customized microfluidic architecture [13], consisting of a polydimethylsiloxane (PDMS) thin membrane able to properly confine the electrolyte and reversibly seal the two electrodes. Copper foils ( $50 \mu\text{m}$ -thick,  $1.5 \text{ cm}^2$  area) were used as electric contacts with FTO, dielectrically insulated by the PDMS membrane. The active area of the cells was  $0.78 \text{ cm}^2$  and

measurements were performed with a 0.22 cm<sup>2</sup> black rigid mask.

**2.2. Characterization.** UV-Visible spectroscopy characterization was carried out using a spectrophotometer (Agilent, Varian Cary 5000) equipped with an integrating sphere to evaluate Kubelka-Munk function  $F(R)$ .  $I$ - $V$  characteristics were measured under the AM1.5G illumination at 100 mW/cm<sup>2</sup> (1 sun) using a class A solar simulator (91195A, Newport) calibrated with a pyranometer (CMP11, Kipp&Zonen), and a Keithley 2440 source measure unit. Incident photon-to-electron conversion efficiency (IPCE) spectra were acquired in DC mode employing a 100 W QTH lamp (Newport) as light source and a 150 mm Czerny Turner monochromator (Omni- $\lambda$  150, Lot-Oriel) without superimposed bias light. Finally Electrochemical Impedance Spectra (EIS) were collected in dark conditions using an electrochemical workstation (760D, CH Instruments) in the frequency range 0.1 Hz–30 kHz at different applied voltages, with superimposed AC signal of 10 mV amplitude. Experimental data of EIS were fitted using an equivalent modeling circuit [17] in order to obtain information about transport and recombination of charges.

### 3. Results and Discussion

Figure 1 shows the structure of the CT1 hemi-squaraine dye molecule. Panel (a) of Figure 2 compares the absorption spectrum of the CT1 in acetonitrile (ACN) solution with the spectra of CT1-sensitized TiO<sub>2</sub> photoanodes at different dipping time intervals. Panel (b) shows the typical IPCE action spectra of CT1-based DSCs for the same sensitization times. Absorbance peaks of CT1-sensitized TiO<sub>2</sub> photoanodes show a monotonous heightening while increasing the sensitization times that can be ascribed to the enhancement of the number of adsorbed dye molecules on the TiO<sub>2</sub> film (Figure 2(a)). On the contrary the maximum IPCE value (55% at 460 nm) has been obtained for a short loading time of only 30 minutes (Figure 2(b)). This result shows that for impregnation times longer than 30 minutes not all the hemi-squaraine molecules attached on TiO<sub>2</sub> surface effectively inject electrons in the TiO<sub>2</sub> conduction band. This fact can be ascribed to their spontaneous aggregation or to an ineffective anchorage of the dye on TiO<sub>2</sub> surface. Since, as previously reported [11], the anchoring of the hemi-squaraine molecule to the (101) anatase surface through the squarate moiety is based on a strong chemical bonding, it is most likely that the ineffective charge transfer for long incubation times is related to the formation of molecular aggregates. The photoanode absorption and the IPCE spectra are broadened and red-shifted with respect to the absorption spectrum of hemi-squaraine in acetonitrile, extending approximately from 375 nm up to 600 nm (Figure 2(a)). The red-shift, which has been also confirmed by DFT *ab initio* calculations, is beneficial for photovoltaic applications [11, 18]. The absorption spectra of CT1-sensitized TiO<sub>2</sub> photoanodes exhibit two well distinguishable peaks: the first one at 414 nm, whose intensity strongly increases until 5 hours of impregnation and

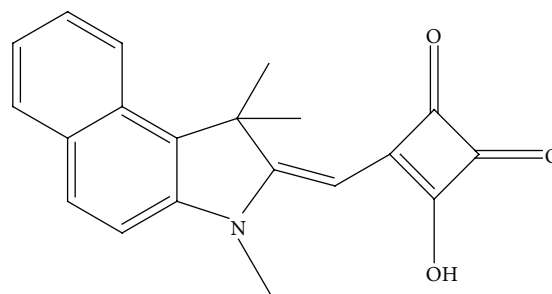


FIGURE 1: Structure of the CT1 hemi-squaraine dye molecule.

the second one at 480 nm, which shows very small variation in intensity with increasing sensitization time. IPCE spectra, instead, show a blue shift, with a lowering and broadening of the peak at 460 nm for loading times longer than 1 hour. The peak at 414 nm is not mirrored in the IPCE spectra, suggesting that its origin is related to H aggregates formation [18], which are unable to inject photogenerated electrons to be collected at the photoanode.

The average photovoltaic parameters (mean values of five cells) obtained from the  $I$ - $V$  measurements varying the sensitization time are summarized in Table 1. For comparison, the data obtained with a reference N719-based cell are also reported in the last row. It has to be noted that the same assembly and characterization procedures have been employed, but the N719 dye concentration in the ethanolic solution and the impregnation time had to be fixed to 0.35 mM and to 18 hours, respectively, in order to achieve the optimal conversion efficiency of 4.83%.

Figure 3 presents a typical photocurrent density-voltage curve of the microfluidic DSCs using the TiO<sub>2</sub>/CT1 electrodes dipped in the dye solution for each sensitization time. The photoconversion efficiency reached the maximum value of 1.75% when the loading time was only 30 minutes long. Increasing the sensitization time to 1, 3, and 5 hours, the conversion efficiencies decreased to 1.66, 1.65, and 1.53%, respectively. The worsening in DSC performance with longer impregnation times is related to the decrement of the short-circuit current density, while open-circuit voltage and fill factor can be considered constant (see Table 1). This behavior, in agreement with the trend evidenced in IPCE action spectra, can be ascribed to a spontaneous aggregation of hemi-squaraine molecules (not effective at 30 minutes). It is particularly interesting to note that, even for a sensitization time as short as 5 minutes, a consistent number of molecules are already attached to the titania surface and are responsible for photocurrent generation. This observation further demonstrates the very efficient and fast linking obtained through the squarate moiety.

Panel (a) of Figure 4 shows a typical Bode representation of impedance phase of the cells by increasing the sensitization time acquired at open circuit voltage condition. Analyzing the Bode plot of EIS (Figure 4(a)), it is possible to notice that the peak related to the electron recombination at the TiO<sub>2</sub>/dye/electrolyte interface shifts to a lower frequency when the sensitization time increases from 5 to 30 minutes

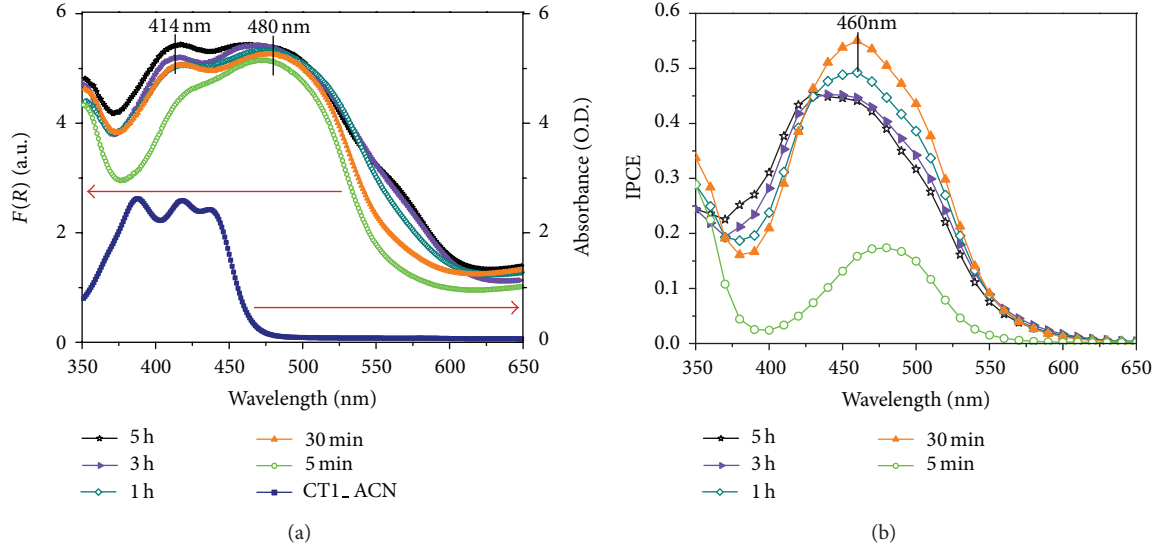


FIGURE 2: (a) UV-Visible absorbance spectra of hemi-squaraine dye in acetonitrile solution and of  $\text{TiO}_2$  photoanodes sensitized in CT1 dye for different time intervals. The values for the CT1 in acetonitrile solution refer to the right-hand axis, whereas the other curves refer to the left-hand axis. (b) IPCE action spectra of CT1-based DSCs for the same sensitization times.

TABLE 1: Average cell parameters (mean values of five cells) evaluated from  $I$ - $V$  characterization. Last row reports the data obtained with a reference N719-based DSC.

Dye	Sensitization time	$J_{sc}$ (mA/cm <sup>2</sup> )	$V_{oc}$ (V)	FF	PCE (%)
CT1	5 min	1.78	0.49	0.61	0.58
CT1	30 min	4.76	0.55	0.67	1.75
CT1	1 h	4.61	0.54	0.67	1.66
CT1	3 h	4.54	0.54	0.68	1.65
CT1	5 h	4.27	0.54	0.66	1.53
N719	18 h	11.56	0.63	0.66	4.83

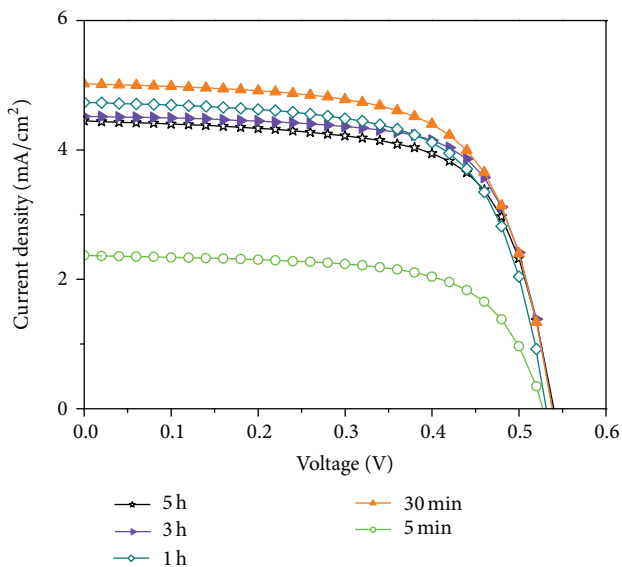


FIGURE 3: Photocurrent density-voltage curves of hemi-squaraine-based DSCs for different sensitization times.

and then it shifts back again to a higher frequency when the loading time further increases from 30 minutes up to 5 hours. These characteristic frequency peaks in Bode plot are inversely proportional to the electron lifetime into the  $\text{TiO}_2$  film [19–21]. Accordingly, the shift to higher (lower) frequency of the peak in Bode phase plot reveals an increase (decrease) of the recombination rate constant or equally a decrease (increase) of the electron lifetime  $\tau$ . The recombination properties were evaluated by fitting EIS experimental data using an equivalent circuit, as described elsewhere [22]. In this modeling circuit the resistance  $R_s$  represents the contact series resistance, the electrolyte-photoanode interface is modeled by a parallel  $R_1//Q_1$ , the parallel  $R_2//Q_2$  stands for the electrolyte-counter-electrode interface, and the Warburg element  $W$  models the diffusion into the electrolyte [23].  $Q_1$  and  $Q_2$  are constant phase elements (CPEs) that are a generalization of common capacitances introduced to better describe the interfaces involving a high-porosity medium. The electron lifetime values calculated using the formula  $\tau = (R_2 Q_2)^{1/\beta_2}$ , where  $\beta_2$  is the exponent of the CPE  $Q_2$ , (reported in Figure 4(b) for different applied bias voltages)

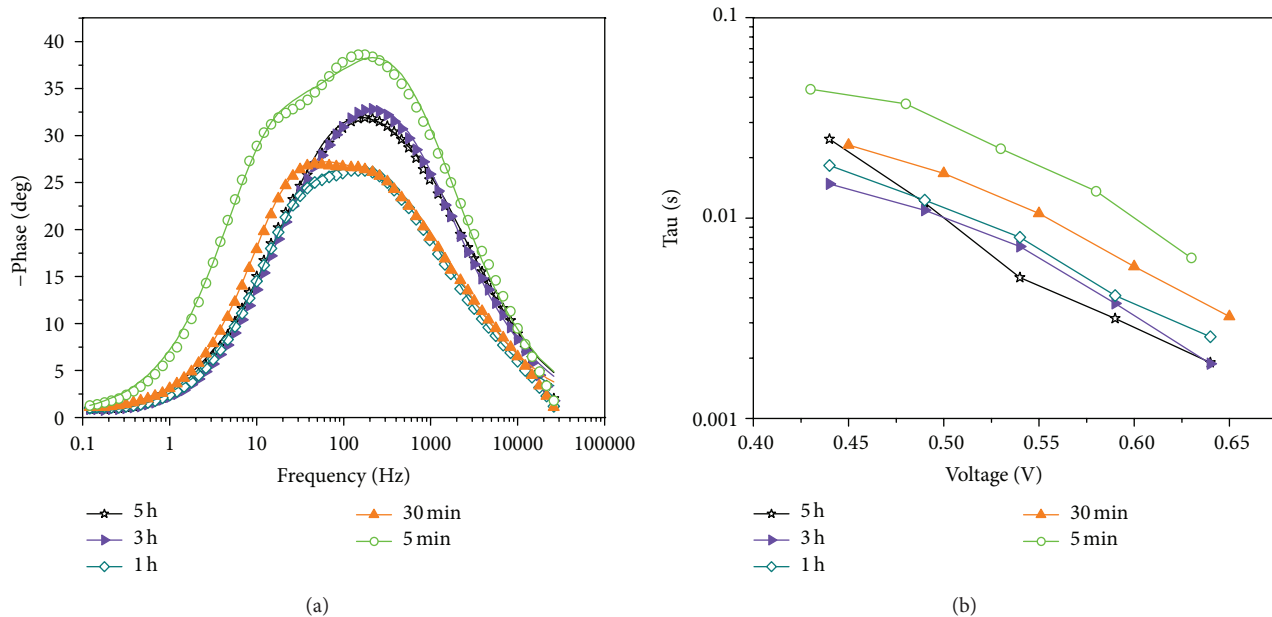


FIGURE 4: (a) Bode plots of hemi-squaraine-based solar cells for different sensitization times measured at open circuit voltage (the symbols represent the experimental data, while the continuous lines correspond to the fitting curves). (b) Electron lifetime evaluated by fitting EIS data.

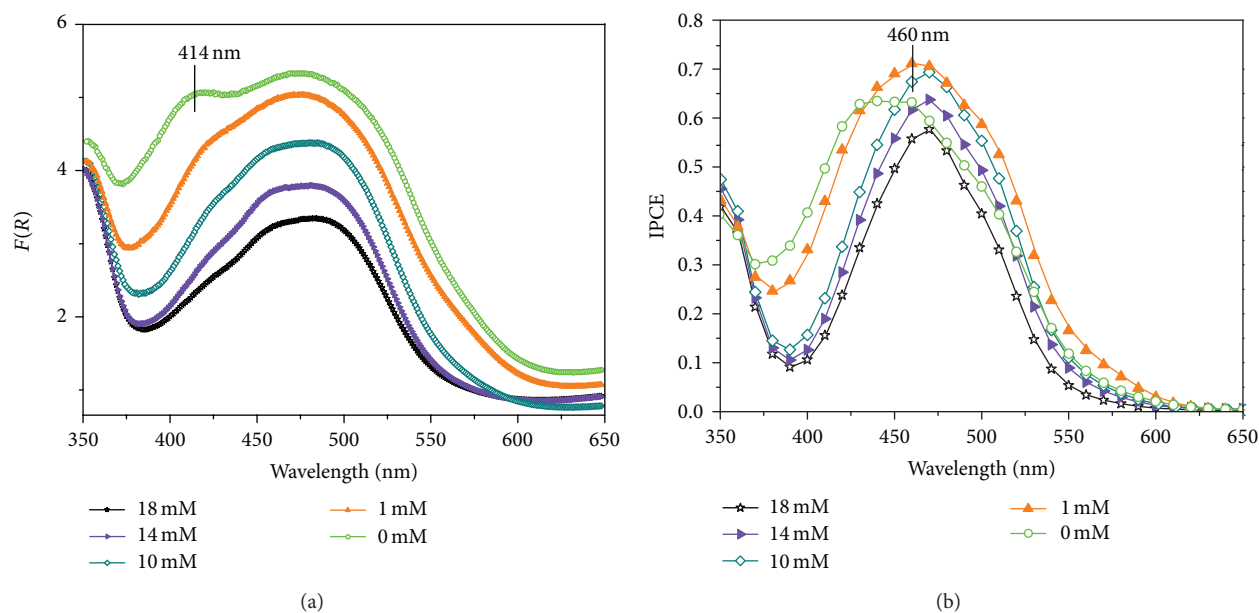


FIGURE 5: (a) UV-Visible absorbance spectra of  $\text{TiO}_2$  photoanodes sensitized in CT1 dye for 1 hour at different CDCA concentrations. (b) IPCE action spectra of CT1-based DSCs for the same sensitization time and CDCA concentrations.

are in agreement with this theoretical prediction for all the sensitization times investigated. In particular, the electron lifetime experiences a monotonous drop while increasing the sensitization time (see panel (b) of Figure 4). This behavior can be ascribed to a spontaneous aggregation of hemi-squaraine dye molecules, phenomenon which leaves a high number of  $\text{TiO}_2$  trap sites not occupied by dye molecules, and so free for electron-hole recombination.

The effect of chenodeoxycholic acid in different concentrations was studied in order to reduce the sensitizer aggregation at the semiconductor surface. The positive effect of the coadsorbent is expected to be more evident for longer sensitization times: for this reason, 1 hour and 3 hours were chosen as dye loading times. Panels (a) and (b) of Figure 5 compare the absorption spectra of  $\text{TiO}_2$  photoanodes sensitized in hemi-squaraine (CT1) dye for 1

hour at different CDCA concentrations and a typical IPCE action spectra of CT1-based DSCs for the same sensitization time and CDCA concentrations, respectively. In Figure 5(a), a lower dye loading induced by CDCA presence is evident; in particular the Kubelka-Munk function of CT1-sensitized  $\text{TiO}_2$  photoanodes experiences a monotonous decrease while enhancing the coadsorbent concentration in the dye solution. This trend is also valid for 3 hours sensitization time (results not reported). It has to be noted that the addition of CDCA in the hemi-squaraine acetonitrile solution is responsible for the disappearance of the shoulder at 414 nm (Figure 5(a)): this confirms the attribution of this absorption peak to dye molecule aggregates on the semiconductor surface. CDCA molecules act as spacers among the CT1 molecules, avoiding dye aggregation and thus facilitating electron injection into the  $\text{TiO}_2$  conduction band. In the IPCE action spectra of Figure 5(b), the beneficial effect of the coadsorbent leads to a rise, narrowing, and slight red-shift of the peak passing from 0 mM to 1 mM of CDCA. Subsequently, further increasing the CDCA concentration, the peak width remains nearly constant, a slight red-shift is still present, but a height reduction occurs. Maximum IPCE (71% at 460 nm) has been obtained for a loading time of 1 hour and a CDCA concentration of 1 mM (Figure 5(b)).

The average photovoltaic parameters (mean values of the five cells) obtained from the  $I$ - $V$  measurements varying the CDCA concentration are summarized in Table 2. The physical quantities in the columns are equal to those reported in Table 1. It has to be pointed out that the differences in the photoconversion efficiency values obtained in the present work (see Tables 1 and 2) and the ones reported by Cicero et al. [11] are first of all due to the different dye and CDCA concentrations and also to the different calibration of the solar simulator. In fact, as recently discussed in the literature [24], the measured DSCs performances are influenced by the employed measurement conditions such as the usage of reference cells. Figure 6 presents a typical photocurrent density-voltage curve of hemi-squaraine-based solar cells for different CDCA concentrations. Maximum photoconversion efficiency of 2.50% was obtained when adding 1 mM CDCA. Further increasing the coadsorbent concentration up to 18 mM, the conversion efficiencies decreased to 1.65%. It is important to highlight that the photoconversion efficiency at 1 hour without CDCA (1.88%) is higher than the one reported in Table 1 (1.66%) since a thicker  $\text{TiO}_2$  layer was deposited onto FTO/glasses. The improvement in DSC performance with a CDCA concentration of 1 mM is related to the enhancement of both the short-circuit photocurrent density ( $J_{sc}$ ) and the open-circuit voltage ( $V_{oc}$ ), while the reduction of the efficiency with higher coadsorbent concentrations (10, 14, and 18 mM) is due to a net decrease of the  $J_{sc}$  originated from a lower dye loading not compensated by an equal increase of the  $V_{oc}$  (see Table 2).

This trend is confirmed by using an impregnation time of 3 hours. In fact, starting from a photoconversion efficiency of 1.67% without CDCA, it subsequently increases up to a value of 2.16% with a CDCA concentration of 1 mM and it finally experiences a decrease down to 1.89% further increasing the CDCA concentration up to 10 mM. The worsening in DSC

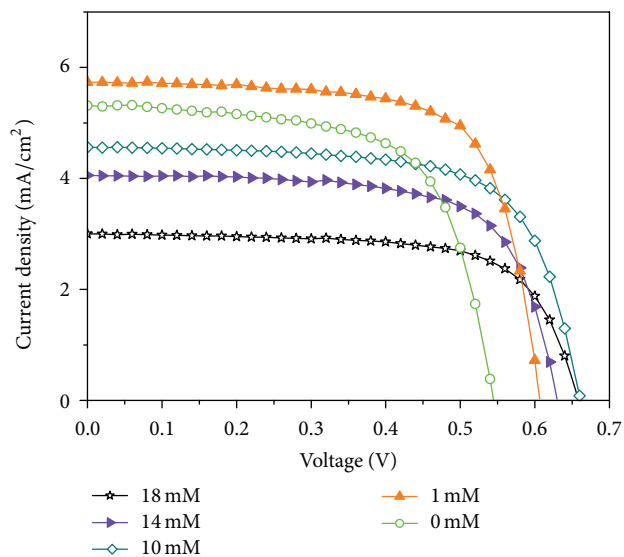


FIGURE 6: Photocurrent density-voltage curves of hemi-squaraine-based DSCs for different CDCA concentrations at an impregnation time of 1 hour.

performance with a longer impregnation time of 3 hours with respect to 1 hour is due to the decrement of the short-circuit current density, while open-circuit voltage can be considered constant (see Table 2).

Increasing the impregnation time, therefore, once the disaggregation has been completed, the acid becomes responsible for a “conflicting mechanism” that prevents the effective attachment of the sensitizer onto the semiconductor surface.

The short-circuit current density increase when using the coadsorbent acid for both the loading time of 1 hour and 3 hours can be attributed to the improved electron injection efficiency [25, 26] following dye disaggregation. The enhancement of the open-circuit voltage, instead, can be explained by analyzing either the  $\tau$  values plotted in panel (b) of Figure 7 and the Bode diagram shown in panel (a) of the same figure. The CDCA molecules dissolved in the dye solution cause an increase of the electron lifetime (Figure 7(b)), a corresponding shift (and an increase) of the middle-frequency peak of the Bode plot toward lower frequency values (Figure 7(a)). The enhancement of the open-circuit voltage, which corresponds to the difference between the free energy of the  $\text{TiO}_2$  electrons and the redox potential of the electrolyte [27], can be therefore linked to a decrease of back electron transfer recombination due to the occupation of  $\text{TiO}_2$  trap sites by the acid molecules.

## 4. Conclusions

The hemi-squaraine anchoring to the  $\text{TiO}_2$  surface has been optimized and characterized by means of an electrical and optical study. The dye sensitization time and the CDCA coadsorbent concentration in the dye solution have been successfully monitored. A maximum photoconversion efficiency of 1.75% for a sensitization time of only 30 minutes without coadsorbent has been obtained, and this value has

TABLE 2: Average cell parameters (mean values of five cells) evaluated from  $I$ - $V$  characterization.

Sensitization time	CDCA (mM)	$J_{sc}$ (mA/cm <sup>2</sup> )	$V_{oc}$ (V)	FF	PCE (%)
1 h	0	5.33	0.54	0.65	1.88
1 h	1	5.90	0.61	0.70	2.50
1 h	10	4.58	0.65	0.69	2.10
1 h	14	3.98	0.65	0.68	1.76
1 h	18	3.76	0.64	0.69	1.65
3 h	0	4.57	0.55	0.66	1.67
3 h	1	4.79	0.60	0.75	2.16
3 h	10	3.96	0.65	0.74	1.89

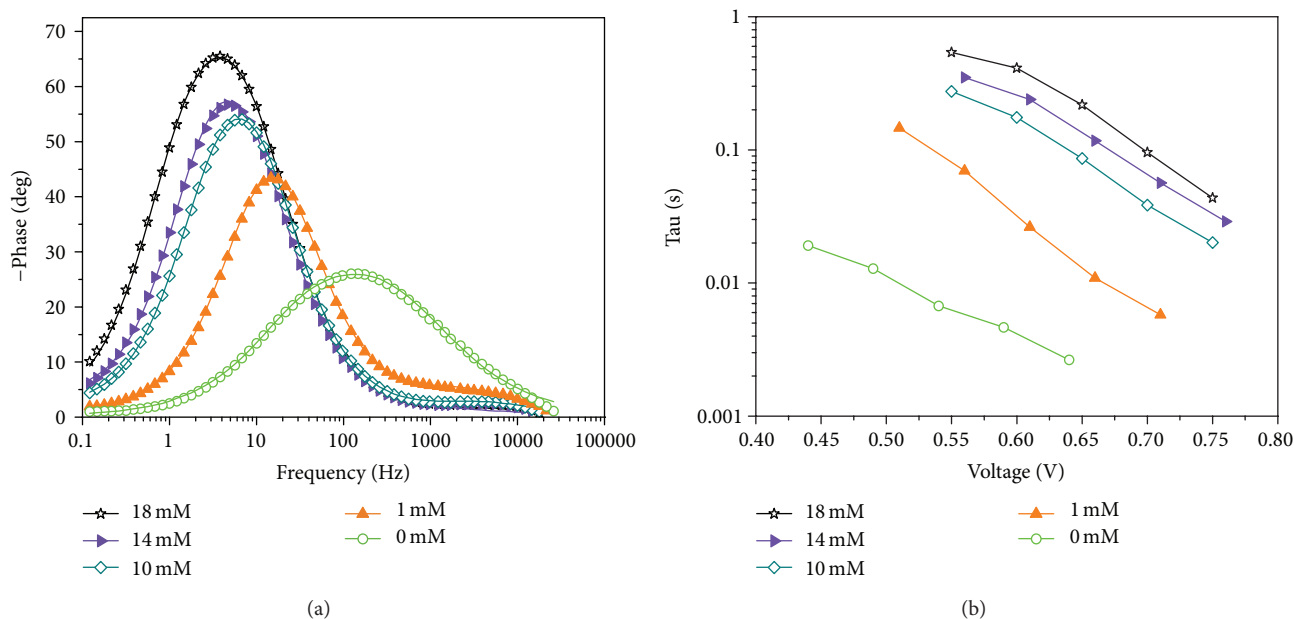


FIGURE 7: (a) Bode plot of CT1-based solar cells for different CDCA concentrations at an impregnation time of 1 hour measured at open circuit voltage (the symbols represent the experimental data, while the continuous lines correspond to the fitting curves). (b) Electron lifetime evaluated by fitting EIS data.

been enhanced up to 2.50% when adding CDCA at 1 mM in the dye solution and fixing the loading time to 1 hour. The optimal DSC performance has been related to the enhancement of both the short-circuit photocurrent density ( $J_{sc}$ ) and the open-circuit voltage ( $V_{oc}$ ). The  $J_{sc}$  increase has been attributed to the improved electron injection efficiency due to the coadsorbent presence, while the  $V_{oc}$  rise has been linked to a decrease of back electron transfer due to the occupation of  $\text{TiO}_2$  trap sites by the acid molecules, as confirmed by the increment of the electron lifetime.

The quite fast linkage of squaric acid moiety anchoring group to the semiconductor surface implies that hemisquaraine dye can lead to technologically easier DSC fabrication, even if the photoconversion efficiency values remain lower with respect to the ones obtained with N719/ $\text{TiO}_2$ -based cells. Finally, the small hemisquaraine dye molecule proposed in this work can be considered as a prototype, and the future employment of new classes of dyes, exhibiting the

same anchoring group and showing an absorption spectrum extended in the entire visible region, turns out to be really promising.

## Conflict of Interests

The authors declare that there is no conflict of interests regarding the publication of this paper.

## Acknowledgments

The authors would like to acknowledge the funding by the Regione Piemonte “Poli di Innovazione” Programme under grant agreement Project “FLEXMAT”; Dr. Claudia Barolo for the helpful discussion, and Mr. Matteo Gerosa for the support in paper preparation.



## References

- [1] B. O'Regan and M. Grätzel, "A low-cost, high-efficiency solar cell based on dye-sensitized colloidal TiO<sub>2</sub> films," *Nature*, vol. 353, no. 6346, pp. 737–740, 1991.
- [2] M. K. Nazeeruddin, C. Klein, P. Liska, and M. Grätzel, "Synthesis of novel ruthenium sensitizers and their application in dye-sensitized solar cells," *Coordination Chemistry Reviews*, vol. 249, no. 13-14, pp. 1460–1467, 2005.
- [3] M. Grätzel, "Recent advances in sensitized mesoscopic solar cells," *Accounts of Chemical Research*, vol. 42, no. 11, pp. 1788–1798, 2009.
- [4] A. Yella, H.-W. Lee, H. N. Tsao et al., "Porphyrin-sensitized solar cells with cobalt (II/III)-based redox electrolyte exceed 12 percent efficiency," *Science*, vol. 334, no. 6056, pp. 629–634, 2011.
- [5] J. Park, C. Barolo, F. Sauvage et al., "Symmetric vs. asymmetric squaraines as photosensitizers in mesoscopic injection solar cells: a structure-property relationship study," *Chemical Communications*, vol. 48, no. 22, pp. 2782–2784, 2012.
- [6] J. Park, G. Viscardi, C. Barolo, and N. Barbero, "Near-infrared sensitization in dye-sensitized solar cells," *Chimia*, vol. 67, no. 3, pp. 129–135, 2013.
- [7] H. Choi, I. Raabe, D. Kim et al., "High molar extinction coefficient organic sensitizers for efficient dye-sensitized solar cells," *Chemistry A*, vol. 16, no. 4, pp. 1193–1201, 2010.
- [8] N. Cai, S.-J. Moon, L. Cevey-Ha et al., "An organic D- $\pi$ -a dye for record efficiency solid-state sensitized heterojunction solar cells," *Nano Letters*, vol. 11, no. 4, pp. 1452–1456, 2011.
- [9] H. Im, S. Kim, C. Park et al., "High performance organic photosensitizers for dye-sensitized solar cells," *Chemical Communications*, vol. 46, no. 8, pp. 1335–1337, 2010.
- [10] T. Inoue, S. S. Pandey, N. Fujikawa, Y. Yamaguchi, and S. Hayase, "Synthesis and characterization of squaric acid based NIR dyes for their application towards dye-sensitized solar cells," *Journal of Photochemistry and Photobiology A*, vol. 213, no. 1, pp. 23–29, 2010.
- [11] G. Cicero, G. Musso, A. Lamberti et al., "Combined experimental and theoretical investigation of the hemi-squaraine/TiO<sub>2</sub> interface for dye sensitized solar cells," *Physical Chemistry Chemical Physics*, vol. 15, no. 19, pp. 7198–7203, 2013.
- [12] A. Calzolari, A. Ruini, and A. Cattellani, "Anchor group versus conjugation: toward the gap-state engineering of functionalized ZnO(10-10) surface for optoelectronic applications," *Journal of the American Chemical Society*, vol. 133, no. 15, pp. 5893–5899, 2011.
- [13] A. Lamberti, A. Sacco, S. Bianco et al., "Microfluidic sealing and housing system for innovative dye-sensitized solar cell architecture," *Microelectronic Engineering*, vol. 88, no. 8, pp. 2308–2310, 2011.
- [14] M. K. Nazeeruddin, A. Kay, I. Rodicio et al., "Conversion of light to electricity by *cis*-X<sub>2</sub>bis(2,2'-bipyridyl-4,4'-dicarboxylate)ruthenium(II) charge-transfer sensitizers (X = Cl<sup>-</sup>, Br<sup>-</sup>, I<sup>-</sup>, CN<sup>-</sup>, and SCN<sup>-</sup>) on nanocrystalline TiO<sub>2</sub> electrodes," *Journal of the American Chemical Society*, vol. 115, no. 14, pp. 6382–6390, 1993.
- [15] L. Vesce, R. Riccitelli, G. Soscia, T. M. Brown, A. Di Carlo, and A. Reale, "Optimization of nanostructured titania photoanodes for dye-sensitized solar cells: study and experimentation of TiCl<sub>4</sub> treatment," *Journal of Non-Crystalline Solids*, vol. 356, no. 37-40, pp. 1958–1961, 2010.
- [16] J. H. Yum, S. J. Moon, R. Humphry-Baker et al., "Effect of coadsorbent on the photovoltaic performance of squaraine sensitized nanocrystalline solar cells," *Nanotechnology*, vol. 19, no. 42, Article ID 424005, 2008.
- [17] R. Harikisun and H. Desilvestro, "Long-term stability of dye solar cells," *Solar Energy*, vol. 85, no. 6, pp. 1179–1188, 2011.
- [18] M. Guo, P. Diao, Y.-J. Ren, F. Meng, H. Tian, and S.-M. Cai, "Photoelectrochemical studies of nanocrystalline TiO<sub>2</sub> co-sensitized by novel cyanine dyes," *Solar Energy Materials and Solar Cells*, vol. 88, no. 1, pp. 23–35, 2005.
- [19] G. Schlichthörl, S. Y. Huang, J. Sprague, and A. J. Frank, "Band edge movement and recombination kinetics in dye-sensitized nanocrystalline TiO<sub>2</sub> solar cells: a study by intensity modulated photovoltage spectroscopy," *Journal of Physical Chemistry B*, vol. 101, no. 41, pp. 8141–8155, 1997.
- [20] G. Schlichthörl, N. G. Park, and A. J. Frank, "Evaluation of the charge-collection efficiency of dye-sensitized nanocrystalline TiO<sub>2</sub> solar cells," *Journal of Physical Chemistry B*, vol. 103, no. 5, pp. 782–791, 1999.
- [21] R. Kern, R. Sastrawan, J. Ferber, R. Stangl, and J. Luther, "Modeling and interpretation of electrical impedance spectra of dye solar cells operated under open-circuit conditions," *Electrochimica Acta*, vol. 47, no. 26, pp. 4213–4225, 2002.
- [22] A. Sacco, A. Lamberti, D. Pugliese et al., "Microfluidic housing system: a useful tool for the analysis of dye-sensitized solar cell components," *Applied Physics A*, vol. 109, no. 2, pp. 377–383, 2012.
- [23] J. R. Macdonald, "Impedance spectroscopy," *Annals of Biomedical Engineering*, vol. 20, no. 3, pp. 289–305, 1992.
- [24] X. Yang, M. Yanagida, and L. Han, "Reliable evaluation of dye-sensitized solar cells," *Energy & Environmental Science*, vol. 6, no. 1, pp. 54–66, 2013.
- [25] A. Ehret, L. Stuhl, and M. T. Spitler, "Spectral sensitization of TiO<sub>2</sub> nanocrystalline electrodes with aggregated cyanine dyes," *Journal of Physical Chemistry B*, vol. 105, no. 41, pp. 9960–9965, 2001.
- [26] J. A. Mikroyannidis, P. Suresh, M. S. Roy, and G. D. Sharma, "New photosensitizer with phenylenebisthiophene central unit and cyanovinylene 4-nitrophenyl terminal units for dye-sensitized solar cells," *Electrochimica Acta*, vol. 56, no. 16, pp. 5616–5623, 2011.
- [27] B. C. O'Regan and J. R. Durrant, "Kinetic and energetic paradigms for dyesensitized solar cells: moving from the ideal to the real," *Accounts of Chemical Research*, vol. 42, no. 11, pp. 1799–1808, 2009.



# The Scientific World Journal

Hindawi Publishing Corporation  
<http://www.hindawi.com>

Volume 2013



Hindawi

- ▶ Impact Factor **1.730**
- ▶ **28 Days** Fast Track Peer Review
- ▶ All Subject Areas of Science
- ▶ Submit at <http://www.tswj.com>